

DESIGN, SYNTHESIS, CRYSTAL STRUCTURE AND BIOLOGICAL EVALUATION OF NOVEL 4-ARYLAMINOQUINAZOLINE DERIVATIVES AS POTENT CYTOTOXIC AGENTS

Xiao Han¹, Liang Liang Chi¹, Wei Tao Qin¹, Ling Hou¹, Zhi Qiang Cai^{1*}, Wen Jie Ren^{2*} and Le Kun Wei³

¹School of Petrochemical Industry, Shenyang University of Technology, Liaoning, Liaoyang, 111003, China

²Key Laboratory for Chemical Drug Research of Shandong Province, Institute of Pharmaceutical Sciences of Shandong Province, Shandong, 250101, China

³Shandong Haiyou Freda Pharmaceutical Co, Ltd, Shandong Linyi, 276000, China

(Received August 25, 2022; Revised June 8, 2023; Accepted June 8, 2023)

ABSTRACT. A series of novel 4-arylaminoquinazoline derivatives were synthesized by five-step reactions, the structure was characterized by IR, ¹H NMR, MS and single crystal X-ray diffraction. The result of **5aX** crystal was as follows: the crystal belongs to the monoclinic system, space group *P21/c* with $a = 12.3637(4)$ Å, $b = 12.7902(2)$ Å, $c = 13.2240(5)$ Å, $\alpha = 90^\circ$, $\beta = 117.030(5)^\circ$, $\gamma = 90^\circ$, $V = 1862.75(12)$ Å³, $Z = 2$, $F(000) = 804.0$, $\mu = 0.095$ mm⁻¹, $S = 1.039$, $R = 0.0569$, $wR = 0.1535$ for 8417 observed reflections with $I > 2\sigma(I)$. The compound **5cX** exhibited an excellent inhibitory effect on the cell line A549 ($IC_{50} < 2.5$ μM) and the drug-resistant cell line H1975 ($IC_{50} < 2.5$ μM) by the biological activity, which were superior to the positive control Zorifertinib (against A549: $IC_{50} = 31.08$ μM; against H1975: $IC_{50} = 64.17$ μM). Molecular docking revealed that the better inhibitory activity of compound **5cX** was owing to the combining EGFR^{WT} and EGFR^{L858R/T790M} by hydrogen bonding. The physicochemical properties of the compounds were predicted by using ADME data analysis, and the results showed that the compounds all obeyed Lipinski's five rules.

KEY WORDS: Quinazoline derivatives, Synthesis, X-ray diffraction, Antitumor activity

INTRODUCTION

Quinazoline is an important pharmacophore as a natural product, and mainly known for its wide range of biological activities [1-3]. Quinazoline compounds have a variety of biological activities such as antitumor, antimalaria, anti-inflammatory, antihypertensive, antiviral and Alzheimer's disease [4-8]. In molecular targeted therapy, quinazoline compounds play an important role which can selectively combine with active molecules in tumor cells to treat the related diseases [9, 10]. For example, 4-arylaminoquinazoline is an early-developed epidermal growth factor receptor tyrosine kinase inhibitor (EGFR-TKIs), which inhibits the growth of tumor cells by highly selective inhibition of epidermal growth factor receptor (EGFR) phosphorylation. Thus, it has been widely studied as an anticancer agent [11, 12].

At present, some quinazoline drugs have been approved as antitumor drugs by the FDA, and widely used in clinical practice, especially in antitumor applications [13]. Since Gefitinib was used for targeted therapy of non-small cell lung cancer as the first generation EGFR-TKIs, it received extensive attention and small molecule targeted drugs had been greatly developed [14]. Currently listed drugs mainly include the first generation of EGFR-TKIs (such as Gefitinib [15], Erlotinib [16], Icotinib [17], etc), the second generation of EGFR-TKIs (such as Afatinib [18], Dacomitinib [19], Canertinib, etc) and the third generation of EGFR-TKIs (such as Osimertinib [20], Poziotinib, etc). However, with the using of small molecule targeted antitumor drugs for a long time, cancer cells would mutate, which resulted in certain drug resistance to the marketing drugs [21]. Moreover, because of the existence of the blood brain barrier, most small molecule

*Corresponding author. E-mail: kahongzqc@163.com, czq0601@126.com

This work is licensed under the Creative Commons Attribution 4.0 International License

inhibitors cannot enter the central nervous system, or be targeted for cancer cells with brain metastases.

As the third-generation EGFR-TKIs, Zorifertinib [22] not only avoids the drug resistance, but also penetrates the blood brain barrier to precisely target non-small cell lung cancer cells with brain metastases, so it is of great research significance. In view of the above situation, our group had synthesized several quinazoline derivatives in order to obtain new quinazoline drugs and studied their antitumor activity [23-25]. In this paper, we used Zorifertinib as the positive control drug, kept its core skeleton as 4-arylaminoquinazoline, and based on the reverse virtual screening of molecular docking and literature analysis. Pyrrolidine (used at 7-position of Cediranib quinazoline) and morpholine (used at 6-position of Gefitinib quinazoline) with similar molecular size were used to replace the heterocyclic ring at the 6-position of Zorifertinib quinazoline in order to produce better targeted binding. The phenyl ring substituent at the 4-position of quinazoline was modified by using different electron-withdrawing substituents and electron-donating substituents, and the density of electron cloud near the phenyl ring was adjusted, from which the substituent more suitable for the active pocket was selected, then designed and synthesized a series of novel 4-arylaminoquinazoline derivatives **5a(X/Y)**~**5c(X/Y)**, which were characterized by IR, ¹H NMR, MS, and the crystal structure of compound **5aX** was characterized by X-ray to determine the spatial structure of the synthesized compounds. Furthermore, the physicochemical properties of the compounds were predicted using ADME data analysis, the inhibitory activity of these compounds on A549 cell line and NCI-H1975 cell line were tested *in vitro* by antitumor activity assay. Simultaneously, molecular docking analysis was performed to explore the possible binding mode between compound **5cX** and EGFR kinase to analyze their mode of action.

EXPERIMENTAL

Chemicals and instruments

All starting materials and reagents were obtained from commercial suppliers without further purification. The melting points of all compounds were determined on a Beijing Taike X-4 microscopy melting point apparatus and were uncorrected. ¹H NMR spectra were obtained on a Bruker Biospin 400 MHz spectrometer using TMS as the internal standard. IR spectra were recorded on a Bruker Platinum ART Tensor II FT-IR spectrometer. MS spectra were acquired on an Esquire-LC mass spectrometer (BrukerDal-tonics, USA) analytical system. The crystal data of compound **5aX** was obtained by Bruker APEX-II CCD surface diffractometer. Both the human lung cancer cell line A549 and the human lung adenocarcinoma cell line NCI-H1975 were purchased from the Shanghai Academy of Life Sciences, Chinese Academy of Sciences, and passed on for cryopreservation by the Pharmacology Department of the Jiangsu Academy of Traditional Chinese Medicine. The inhibition rate data of compounds on cells were obtained from RT-6100 microplate reader.

Synthesis and characterization of 7-methoxy-4-(phenylamino)quinazolin-6-yl acetate (3a)

7-Methoxy-4-oxo-3,4-dihydroquinazolin-6-yl acetate (1.01 g, 4.33 mmol), triethylamine (0.76 g, 7.49 mmol) and phosphorus oxychloride (1.74 g, 11.34 mmol) were added in a flask, and dissolved in toluene (12 mL). The mixture was stirred at 80 °C. After 6 h, aniline (0.45 g, 4.79 mmol) was dropwise added to the reaction solution and then stirred for 5 h. After the reaction was completed, the toluene in the reaction mixture was evaporated under reduced pressure, and isopropanol (20 mL) was added and stirred for 2 h, then filtered under reduced pressure, and dried to obtain **3a** (1.28 g, yield: 86%) as a white solid. Mp: 178.7-180.5 °C (dec); ¹H NMR (DMSO-*d*₆): 11.64 (s, 1H, H_{pyrimidine}), 8.89 (d, *J* = 15.2 Hz, 2H, H_{arom}), 7.71 (d, *J* = 8.0 Hz, 2H, H_{arom}), 7.59 (s, 1H, NH), 7.49 (t, *J* = 7.6 Hz, 2H, H_{arom}), 7.33 (t, *J* = 7.2 Hz, 1H, H_{arom}), 4.01 (s, 3H, OMe), 2.39 (s, 3H, CMe); IR (KBr; cm⁻¹): 1777 (vs), 1628 (m), 1560 (m), 1427 (s), 1217 (s), 1153 (s).

Synthesis and characterization of 7-methoxy-4-(phenylamino)quinazolin-6-ol (4a)

Aqueous ammonia (2 mL) was dropwise added to the mixture of 7-methoxy-4-(phenylamino)quinazolin-6-ol **3a** (1.35 g, 5.05 mmol) and methanol (5 mL) in an ice bath, which was then stirred for 3 h at the room temperature. The solid was filtered, washed with a mixture of cold methanol and water, then dried to obtain **4a** (1.04 g, yield: 89%) as a white solid. Mp: 279.2-281.1 °C (dec); ¹H NMR (DMSO-*d*₆): 9.37 (s, 1H, H_{arom}), 8.43 (s, 1H, H_{pyrimidine}), 7.89-7.70 (m, 3H, H_{arom}), 7.36 (t, *J* = 7.6 Hz, 2H, H_{arom}), 7.20 (s, 1H, NH), 7.07 (t, *J* = 7.2 Hz, 1H, H_{arom}), 3.98 (s, 3H, OMe); IR (KBr, cm⁻¹): 3390 (m), 1605 (m), 1579 (m), 1443 (s), 1243 (s), 1067 (s).

Synthesis and characterization of pyrrolidine-1-carbonyl chloride (X)

In a round bottom flask (50 mL), the pyrrolidine (0.25 g, 3.52 mmol) was added to dichloromethane (5 mL), then triphosgene (0.86 g, 3.66 mmol) and pyridine (0.84 g, 10.87 mmol) were slowly added in the mixture at 0 °C. The mixture was stirred for 5 h at room temperature. After the completion, the dichloromethane was evaporated under reduced pressure to obtain **X** (0.42 g, yield: 89%) as a yellow solid. The next reaction was proceeded directly without further treatment.

Synthesis and characterization of 7-methoxy-4-(phenylamino)quinazolin-6-yl pyrrolidine-1-carboxylate (5aX)

The pyrrolidine-1-carbonyl chloride **X** (0.42 g, 3.14 mmol) and *N,N*-dimethylformamide (25 mL) were added in a flask, then the intermediate 7-methoxy-4-(phenylamino)quinazolin-6-ol **4a** (0.83 g, 3.11 mmol) and anhydrous potassium carbonate (0.85 g, 6.16 mmol) were added in the mixture at 0 °C, and the reaction was continued at room temperature for 5 h. After the completion, the solvent was removed under reduced pressure, and deionized water was added to the precipitate, after suction filtration to obtain **5aX** (0.91 g, yield: 80%) as a yellow solid. Mp: 235.8-237.7 °C (dec); ¹H NMR (DMSO-*d*₆): 9.56 (s, 1H, H_{pyrimidine}), 8.55 (s, 1H, H_{arom}), 8.35 (s, 1H, H_{arom}), 7.90 - 7.82 (m, 2H, H_{arom}), 7.38 (t, *J* = 7.5 Hz, 2H, H_{arom}), 7.32 (s, 1H, NH), 7.10 (dd, *J* = 7.3, 6.6 Hz, 1H, H_{arom}), 3.94 (s, 3H, OMe), 3.56 (t, *J* = 6.7 Hz, 2H, H_{pyrrolidine}), 3.37 (t, *J* = 6.6 Hz, 2H, H_{pyrrolidine}), 2.03 - 1.81 (m, 4H, H_{pyrrolidine}); IR (KBr, cm⁻¹): 3321 (m), 2975 (s), 1696 (vs), 1604 (m), 1426 (s), 1139 (s), 1057 (s); MS (ESI⁺): [M+H]⁺ = 365.2.

Synthesis and characterization of 4-((4-fluoro-2-methylphenyl)amino)-7-methoxyquinazolin-6-yl pyrrolidine-1-carboxylate (5bX)

Pyrrolidine-1-carbonyl chloride **X** (0.40 g, 2.99 mmol), anhydrous potassium carbonate (0.80 g, 5.80 mmol) and *N,N*-dimethylformamide (25 mL) were added in a flask, then the intermediate 4-((4-fluoro-2-methylphenyl)amino)-7-methoxyquinazolin-6-ol **4b** (0.88 g, 2.94 mmol) was added in the mixture at 0 °C, and the reaction was continued at room temperature for 5 h. After the completion, the solvent was removed under reduced pressure, and deionized water was added to the precipitate, after suction filtration to obtain **5bX** (1.00 g, yield: 85%) as a yellow solid. Mp: 229.1-230.4 °C (dec); ¹H NMR (DMSO-*d*₆): 9.40 (s, 1H, H_{pyrimidine}), 8.36 (s, 2H, NH+H_{arom}), 7.30 (s, 4H, H_{arom}), 3.94 (s, 3H, OMe), 3.56 (s, 2H, H_{pyrrolidine}), 3.36 (s, 2H, H_{pyrrolidine}), 2.18 (s, 3H, CH₃-Ar), 1.92 (s, 4H, H_{pyrrolidine}); IR (KBr, cm⁻¹): 3357 (m), 2979 (s), 1593 (m), 1431 (s), 1132 (s), 1050 (s).

Synthesis and characterization of 7-methoxy-4-((4-methoxyphenyl)amino)quinazolin-6-yl pyrrolidine-1-carboxylate (5cX)

Pyrrolidine-1-carbonyl chloride **X** (0.50 g, 3.74 mmol), anhydrous potassium carbonate (1.0 g, 7.25 mmol) and *N,N*-dimethylformamide (25 mL) were added in a flask, then the intermediate 7-

methoxy-4-((4-methoxyphenyl)amino)quinazolin-6-ol **4c** (1.00 g, 3.36 mmol) was added in the mixture at 0 °C, and the reaction was continued at room temperature for 5 h. After the completion, the solvent was removed under reduced pressure, and deionized water was added to the precipitate, after suction filtration to obtain **5cX** (1.15 g, yield: 86%) as a yellow solid. Mp.: 248.2-250.4 °C (dec); ¹H NMR (DMSO-*d*₆): 9.47 (s, 1H, H_{pyrimidine}), 8.49 (s, 1H, H_{arom}), 8.30 (s, 1H, H_{arom}), 7.71 (d, *J* = 8.3 Hz, 2H, H_{arom}), 7.29 (s, 1H, NH), 6.96 (d, *J* = 8.4 Hz, 2H, H_{arom}), 3.94 (s, 3H, OMe), 3.77 (s, 3H, OMe), 3.56 (s, 2H, H_{pyrrolidine}), 3.37 (s, 2H, H_{pyrrolidine}), 2.00 - 1.84 (m, 4H, H_{pyrrolidine}); IR (KBr, cm⁻¹): 3349 (m), 2951 (s), 1695 (vs), 1629 (m) 1433 (s), 1137 (s), 1071 (s); MS (ESI⁺): [M+H]⁺ = 395.1.

Synthesis of morpholine-4-carbonyl chloride (Y)

In a round bottom flask (50 mL), the morpholine (0.20 g, 2.32 mmol) was added to dichloromethane (5 mL), then triphosgene (0.69 g, 2.33 mmol) and pyridine (0.55 g, 6.96 mmol) were slowly added in the mixture at 0 °C, then heated to room temperature and stirred for 5 h. After the completion, the dichloromethane was evaporated under reduced pressure to obtain **Y** (0.30 g, yield: 86%) as a yellow solid. And it was required to proceed directly to the next reaction without further treatment.

Synthesis and characterization of 7-methoxy-4-(phenylamino)quinazolin-6-yl morpholine-4-carboxylate (5aY)

In a round bottom flask (50 mL), the morpholine-4-carbonyl chloride **Y** (0.30 g, 2.00 mmol) was added to *N,N*-dimethylformamide (25 mL), then the intermediate 7-methoxy-4-(phenylamino)quinazolin-6-ol **4a** (0.52 g, 1.95 mmol) and anhydrous potassium carbonate (0.7 g, 5.07 mmol) were added in the mixture at 0 °C, and the reaction was continued at room temperature for 5 h. After the completion, the solvent was removed under reduced pressure, and deionized water was added to the precipitate, after suction filtration to obtain of **5aY** (0.68 g, yield: 92%) as a white solid. Mp: 119.4-120.7 °C (dec); ¹H NMR (DMSO-*d*₆): 9.59 (s, 1H, H_{pyrimidine}), 8.55 (s, 1H, H_{arom}), 8.36 (s, 1H, H_{arom}), 7.84 (s, 2H, H_{arom}), 7.38 (s, 2H, H_{arom}), 7.32 (s, 1H, NH), 7.11 (s, 1H, H_{arom}), 3.95 (s, 3H, OMe), 3.67 (s, 6H, H_{morpholine}), 3.46 (s, 2H, H_{morpholine}); IR (KBr, cm⁻¹): 3359 (m), 2974 (s), 1696 (vs), 1606 (m), 1447 (s), 1111 (s), 1067 (s); MS (ESI⁺): [M+H]⁺ = 381.2.

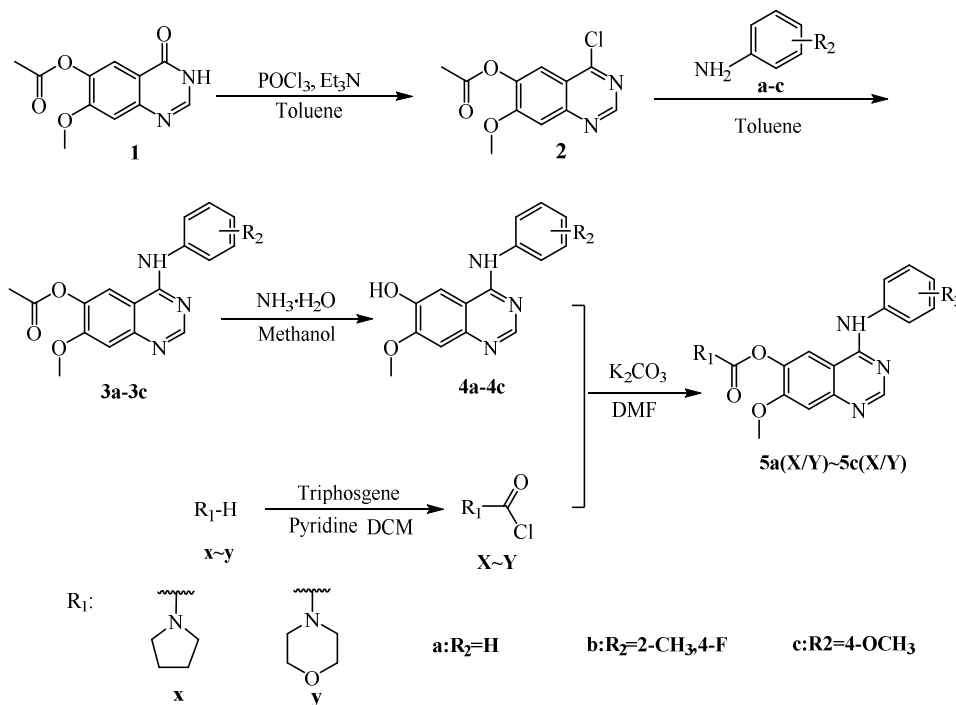
Synthesis and characterization of 4-((4-fluoro-2-methylphenyl)amino)-7-methoxyquinazolin-6-yl morpholine-4-carboxylate (5bY)

Morpholine-4-carbonyl chloride **Y** (0.45 g, 3.01 mmol), anhydrous potassium carbonate (0.7 g, 5.07 mmol) and *N,N*-dimethylformamide (25 mL) were added in a flask, then the intermediate 4-((4-fluoro-2-methylphenyl)amino)-7-methoxyquinazolin-6-ol **4b** (0.90 g, 3.00 mmol) was added in the mixture at 0 °C, and the reaction was continued at room temperature for 5 h. After the completion, the solvent was removed under reduced pressure, and deionized water was added to the precipitate, after suction filtration to obtain of **5bY** (1.03 g, yield: 83%) as a yellow solid. Mp: 119.4-120.7 °C (dec); ¹H NMR (DMSO-*d*₆): 9.44 (s, 1H, H_{pyrimidine}), 8.36 (s, 1H, NH), 8.24 (s, 1H, H_{arom}), 7.30 (s, 2H, H_{arom}), 7.17 (d, *J* = 9.7 Hz, 1H, H_{arom}), 7.08 (t, *J* = 8.6 Hz, 1H, H_{arom}), 3.95 (s, 3H, OMe), 3.67 (s, 6H, H_{morpholine}), 3.46 (s, 2H, H_{morpholine}), 2.17 (s, 3H, CH₃-Ph); IR (KBr, cm⁻¹): 3551 (m), 2980 (s), 2941 (s), 1713 (vs), 1620 (m), 1465 (s), 1112 (s), 1068 (s).

Synthesis and characterization of 7-methoxy-4-((4-methoxyphenyl)amino)quinazolin-6-yl morpholine-4-carboxylate (5cY)

Morpholine-4-carbonyl chloride **Y** (0.40 g, 2.67 mmol), anhydrous potassium carbonate (0.8 g, 5.80 mmol) and *N,N*-dimethylformamide (25 mL) were added in a flask, then the intermediate 7-methoxy-4-((4-methoxyphenyl)amino)quinazolin-6-ol **4c** (0.78 g, 2.62 mmol) was added in the

mixture at 0 °C, and the reaction was continued at room temperature for 5 h. After the completion, the solvent was removed under reduced pressure, and deionized water was added to the precipitate, after suction filtration to obtain **5cY** (1.00 g, yield: 92%) as a yellow solid. Mp: 236.8-238.3 °C (dec); ¹H NMR (DMSO-*d*₆): 9.51 (s, 1H, H_{pyrimidine}), 8.49 (s, 1H, H_{arom}), 8.32 (s, 1H, H_{arom}), 7.70 (d, *J* = 8.9 Hz, 2H, H_{arom}), 7.29 (s, 1H, NH), 6.97 (s, 2H, H_{arom}), 3.95 (s, 3H, OMe), 3.77 (s, 3H, OMe), 3.68 (s, 6H, H_{morpholine}), 3.47 (s, 2H, H_{morpholine}); IR (KBr, cm⁻¹): 3356 (m), 2912 (s), 1697 (vs), 1628 (m), 1454 (s), 1111 (s), 1067 (s); MS (ESI⁺): [M+H]⁺ = 411.2.



Scheme 1. The synthetic route of target compounds.

Crystal structure determination

The target compound **5aX** was dissolved in the mixed solution of methanol and dichloromethane ($V_{\text{MeOH}}: V_{\text{DCM}} = 2:1$), and the solvent was slowly evaporated until regular needle-like crystals grow after 10 days. A colorless single crystal ($\text{C}_{41}\text{H}_{44}\text{N}_8\text{O}_7$) measuring $0.12 \times 0.11 \times 0.10 \text{ mm}^3$ was placed on a Bruker APEX-II CCD surface diffractometer. The data were collected by using MoK α radiation ($\lambda = 0.71073 \text{ \AA}$). In the range of $3.458^\circ \leq 2\theta \leq 58.850^\circ$, a total of 26819 independent diffraction points were scanned and collected while maintaining the temperature of 100 K, and 8417 of them could be used for calculation. The scheme was solved using the ShelXT structure, the structure was solved by using the inherent phase and optimized by the least square method of the ShelXL [26] improved package. Final deviation factors ($I > 2\sigma(I)$): $R_1 = 0.0569$, $wR_2 = 0.1476$, and final deviation factors (all data): $R_1 = 0.0663$, $wR_2 = 0.1535$ ($w = 1/[\sigma^2(F_o^2) + (P)^2 + P]$). The largest difference electron density (largest diff): $(\Delta\rho)_{\text{max}} = 0.70 \text{ e/\AA}^3$ and $(\Delta\rho)_{\text{min}} = -0.40 \text{ e/\AA}^3$. The data can be obtained from the Cambridge Crystallographic Data Centre via <http://summary.ccdc.cam.ac.uk/structure-summary-form>.

In vitro antitumor activity assay

Cell cryovials were placed in a water bath at 37 °C, and shaken for 1-2 min until the cryovials were thawed. The supernatant was obtained after centrifuging (5 min) at 800 rpm. A small amount of culture medium containing 10% calf serum was added to it, and the cell mass was blown to uniformity with a pipette. Then, the obtained was transferred to a culture flask with 10-15 mL culture medium and keep in a 37 °C, 5% CO₂ incubator. One day before the test, A549 cells were seeded in 96-well cell plates at 1000 cells per well. And H1975 cells were seeded in a 96-well cell plate at 2000 cells per well, and 80 µL of cell suspension was seeded in each well. The cell plate was placed in a 37 °C, 5% CO₂ incubator for 12 h. On the day of the experiment, according to the compound arrangement diagram, 20 µL/well of the prepared compound working solution was added to the cell plate, and the cell plates were incubated at 37 °C in a 5% CO₂ incubator for 72 h in the dark. After the incubation, 10 µL/well of CCK-8 reagent was added to the cell solution, and then placed in a 37 °C, 5% CO₂ incubator for 1 h. The absorbance (OD) was measured with a microplate reader at a wavelength of 450 nm, and the inhibition ratio was calculated. The specific calculation formula is: IR% = (sample wells OD - control wells OD) / (control wells OD - blank wells OD) × 100%. According to the absorbance value, the IC₅₀ value of the corresponding compounds were calculated and converted by the Bliss method.

Molecular docking study

The binding mode of compound **5cX** was explained by selecting the protein structures of EGFR^{WT} and EGFR^{L858R/T790M} as receptors, which are retrieved from the RCSB protein database (RCSB.org) (PDB IDs: 2GS7 EGFR^{WT} [27] and 5EDP EGFR^{L858R/T790M} [28]) and the specific steps are as follows. First, water was removed from the receptor structures. Second, the hydrogens of crystal structures of the receptors and ligands were added, and the coordinate files of the individual proteins and ligands were generated into PDBQT files by using autodocktools-1.5.6 (The Scripps Research Institute, La Jolla, California, USA). Finally, the protein binding sites were covered by a grid box, after saving the file and performing molecular docking. The visual geometric simulation graph was drawn by PyMOL [29] after checking the docking results.

ADME properties

The drug properties of the compounds and the positive control drug were predicted by the Swiss ADME which is the free web tool to evaluate physicochemical properties, lipophilicity, water Solubility, pharmacokinetics, druglikeness and medicinal chemistry [30]. The predicted directions of drug properties are divided into six aspects: the pink area represents the optimal range for each property (lipophilicity: XLOGP3 between -0.7 and +5.0, size: MW between 150 and 500 g/mol, polarity: TPSA between 20 and 130 Å², solubility: log S not higher than 6, saturation: fraction of carbons in the sp³ hybridization not less than 0.25, and flexibility: no more than 9 rotatable bonds).

RESULTS AND DISCUSSION

Synthesis and spectra analysis

The synthetic methods of compounds **5a(X/Y)**-**5c(X/Y)** are shown in Scheme 1. 4-Chloro-7-methoxyquinazoline-6-acetate (**2**) was synthesized with Commercially available 7-methoxy-4-oxo-3,4-dihydroquinazolin-6-yl acetate (**1**) by chlorination reaction, and substituted aniline (**a-c**) were directly added to produce intermediate 7-methoxy-4-(substituted aniline) quinazoline-6-acetate (**3a-3c**). The key intermediates 7-methoxy-4-(substituent aniline)quinazolin-6-ol **4a-4c** were synthesized by hydrolysis reaction with intermediates **3a-3c**. The compound **X-Y** were prepared by acylation reaction with compounds **X-Y** and triphosgene. After the substitution

reaction between compounds X~Y and the key intermediates 4a~4c, the target compounds 5a(X/Y)~5c(X/Y) were synthesized. The structures of the target compounds were confirmed by IR, ¹H NMR and MS, and the crystal structure of compound 5aX was established by X-ray diffraction analysis.

Crystal structure

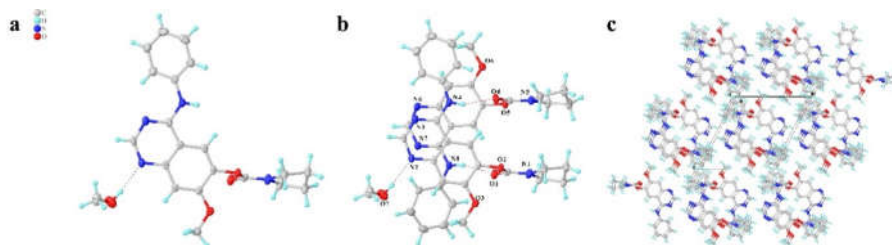


Figure 1. (a) Molecular structure of compound 5aX, (b) intermolecular hydrogen bonding diagram of 5aX and (c) a packing diagram of 5aX.

Table 1. Crystal data for the compound 5aX.

Parameter	Value	Parameter	Value
Crystal size, mm ³	0.12×0.11×0.1	<i>V</i> , Å ³	1862.75(12)
Formula	C ₄₁ H ₄₄ N ₈ O ₇	<i>Z</i>	2
<i>F</i> _w	760.84	<i>D</i> _c , g·cm ⁻³	1.356
<i>T</i> , K	100.0(4)	<i>μ</i> , mm ⁻¹	0.095
Crystal system	Monoclinic	<i>F</i> (000)	804.0
Space group	<i>P</i> 21/ <i>c</i>	GOF on <i>F</i> ²	1.039
<i>a</i> , Å	12.3637(4)	Reflection/unique	26819/8417
<i>b</i> , Å	12.7902(2)	<i>R</i> ₁ , <i>wR</i> ₂ [<i>I</i> > 2σ(<i>I</i>)]	0.0569, 0.1476
<i>c</i> , Å	13.2240(5)	<i>R</i> ₁ , <i>wR</i> ₂ (all data)	0.0663, 0.1535
<i>α</i> , °	90		
<i>β</i> , °	117.030(5)		
<i>γ</i> , °	90		

$$R_1 = \frac{\sum(|F_o| - |F_c|)}{\sum|F_o|} \quad wR_2 = \frac{[\sum w(F_o^2 - F_c^2)^2 / \sum w(F_o^2)]^{1/2}}$$

Table 2. Hydrogen bond lengths (Å) and bond angles (°) of compound 5aX.

D-H...A	d(D-H)/Å	d(H-A)/Å	d(D-A)/Å	D-H-A/°
N(8)-H(8)A...O(1)	0.86	2.11	2.931(4)	160.2
N(4)-H(4)...O(4)	0.86	2.08	2.911(4)	160.9
O(7)-H(7)...N(2)	0.82	2.03	2.847(5)	171.5

Symmetry code: -x, y+1/2, -z.

The structure of compound 5aX was further confirmed by single crystal X-ray diffraction analysis. The crystal structure of 5aX belongs to the monoclinic system which crystallized in space group *P*21/*c*. The molecular single crystal diagram, hydrogen bond diagram of compound 5aX and the unit cell stacking diagram are shown in Figure 1. Crystal data for the compound 5aX are given in Table 1. Hydrogen bond lengths (Å) and bond angles (°) of compound 5aX are given in Table 2. CCDC 2102043 contains the supplementary data for this paper. As shown in the data, the chemical bond lengths of compound 5aX are all within the normal range of single and double

bonds, and the N4 atom has sp² hybridization. The C-O bond near one end of the benzene ring is affected by the conjugation of the benzene ring, and the oxygen atom is biased to the side of the benzene ring. The carbonyl group has a strong electron withdrawing ability, while the nitrogen atom is biased towards the carbonyl side. Meanwhile, the bond angle is in the lowest energy state in the corresponding chemical environment, and the chemical structure is stable. Due to the conjugation of the benzene ring and the pyrimidine ring and the influence of steric hindrance, among the bond angles with N as the central atom, the bond angle of C14-N4-C15 is 128.4°(3), which is much larger than the three bond angles [126.6°(3), 118.0°(12), 115.4°(12)] with N1 as the central atom, and the bond angle of C34-N8-C35 is 127.7°(3), which is much larger than the three bond angles [126.1°(3), 120.9°(3), 113.0°(3)] with N5 as the central atom. At the same time, the twist angles of C12-O3-C7-C6 [175.0°(3)] and C12-O3-C7-C8 [5.8°(5)] are small, which proves the methoxy group at the 7-position of the quinazoline core is almost coplanar with the quinazoline ring. As shown in Figure 2, molecular packing and hydrogen bonding in the unit cell are depicted, with 3 hydrogen bond acceptors in each C₄₁H₄₄N₈O₇ molecule. Details as follows: N4 on the 4-position of quinazoline forms a hydrogen bond with O4 on the carbonyl group; N8 forms a hydrogen bond with O1 on the carbonyl group; H7 on methanol forms a hydrogen bond with the N2 on the 1-position of quinazoline. Thus, a complex spatial network stacking structure is formed.

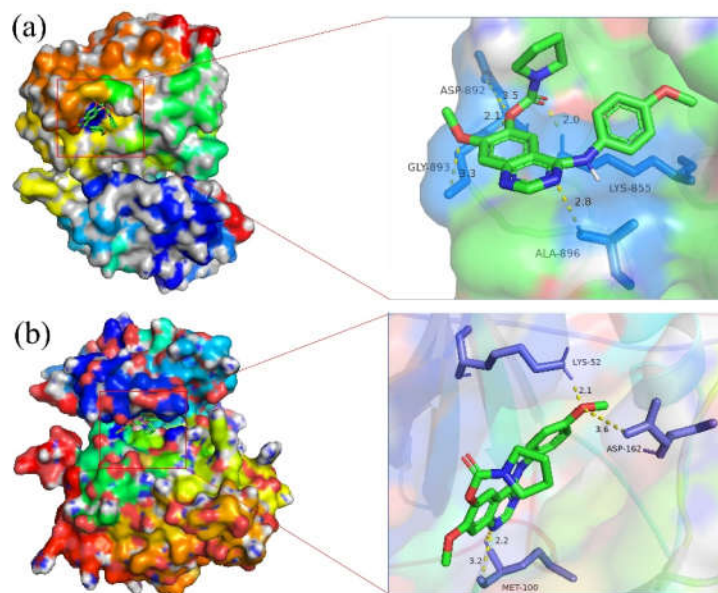


Figure 2. (a) 3D model of compound **5cX** bound to EGFR^{WT} (PDB code: 2GS7). (b) 3D model of compound **5cX** bound to EGFR^{L858R/T790M} (PDB code: 5EDP).

Antitumor activity and structure-activity relationship

The antitumor activities of compounds against human lung cancer cells A549 and human lung adenocarcinoma cells H1975 were evaluated by CCK-8 method *in vitro* with Zorifertinib as the positive control, the inhibitory effects of the compounds against A549 and H1975 are shown in Table 3. For the human lung cancer cell line A549, part of the target derivatives showed a certain inhibitory activity. Among them, compound **5cX** (R₁ = pyrrolidine, R₂ = 4-OCH₃) had significant

inhibitory activity, and its inhibition rate was 97.09%, which was better than that of Zorifertinib (the inhibition rate: 62.14%) and compound **5cX** (R_1 = pyrrolidine, R_2 = 4-OCH₃) was also better than compound **5aX** (R_1 = pyrrolidine, R_2 = H, inhibition rate: 24.96%). The inhibition rate of compound **5bX** (R_1 = pyrrolidine, R_2 = 2-CH₃, 4-F) was 59.94%, which was close to that of the Zorifertinib (inhibition rate: 62.14%), and had a certain inhibitory effect. Most of the target derivatives were less sensitive to the drug-resistant cell line H1975, and the inhibition rate was mostly lower than that of Zorifertinib (49.60%). In order to further study the antitumor activity of compound **5cX** *in vitro* on cell lines A549 and H1975, the half inhibitory concentration (IC₅₀) of compound **5cX** on A549 and H1975 was tested with Zorifertinib as a positive control and the results are shown in Table 4. For A549 cell line, compound **5cX** (IC₅₀ < 2.5 μM) showed a more significant antitumor activity than Zorifertinib (IC₅₀ = 31.08 μM). For H1975 cell line, the IC₅₀ value of compound **5cX** was less than 2.5 μM, and the inhibitory activity was also better than that of Zorifertinib (IC₅₀ = 64.17 μM).

Table 3. Inhibitory rates of Zorifertinib and its derivatives on tumor cells cultured *in vitro*.

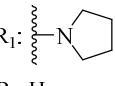
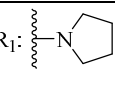
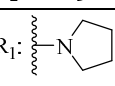
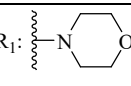
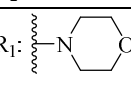
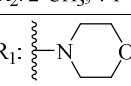
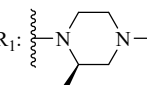
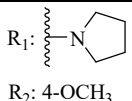
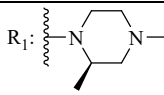
Series	Compd.	Structure	Inhibition rate (%)	
			A549	H1975
X	5aX	 R_1 : R_2 : H	24.96	28.47
	5bX	 R_1 : R_2 : 2-CH ₃ , 4-F	59.94	13.02
	5cX	 R_1 : R_2 : 4-OCH ₃	97.09	22.74
Y	5aY	 R_1 : R_2 : H	39.05	31.02
	5bY	 R_1 : R_2 : 2-CH ₃ , 4-F	23.25	10.77
	5cY	 R_1 : R_2 : 4-OCH ₃	22.47	17.62
	Zorifertinib	 R_1 : R_2 : 2-F, 3-Cl	62.14	49.60

Table 4. Inhibitory activity of target derivatives **5cX**.

Comp.	Structure	IC ₅₀ (μM)	
		A549	H1975
5cX	 R ₁ :  R ₂ : 4-OCH ₃	<2.5	<2.5
Zorifertinib	 R ₁ :  R ₂ : 2-F, 3-Cl	31.08	64.17

Molecular docking of compounds **5cX**

In order to further clarify the binding mode of compound **5cX** to EGFR (EGFR^{WT} and EGFR^{L858R/T790M}), the binding mode of compound **5cX** to EGFR was simulated by molecular docking. The PyMOL software was combined with EGFR^{WT} protein (PDB Code: 2GS7) and EGFR^{L858R/T790M} mutant protein (PDB Code: 5EDP). Molecular docking simulation results were shown in Figure 2. In the EGFR^{WT} binding model, the Nitrogen atom at position 3 of quinazoline ring bound to the ALA-896 residue by hydrogen bonding, the ester group at position 6 of quinazoline formed hydrogen bonds with ASP-892 residue and LYS-855 residue, and the oxygen atom of the 7-position methoxy group was hydrogen-bonded to GLY-893. In the EGFR^{L858R/T790M} binding model, the quinazoline ring is hydrogen-bonded to the MET-100 residue. Notably, the oxygen atom of the methoxy group on the 4-position bound to the LYS-52 residue and the ASP-162 residue through hydrogen bond, and it may result from the excellent inhibitory activity after the 4-position is substituted by *p*-methoxyaniline (compound **5cX**).

Physicochemical and ADME parameters

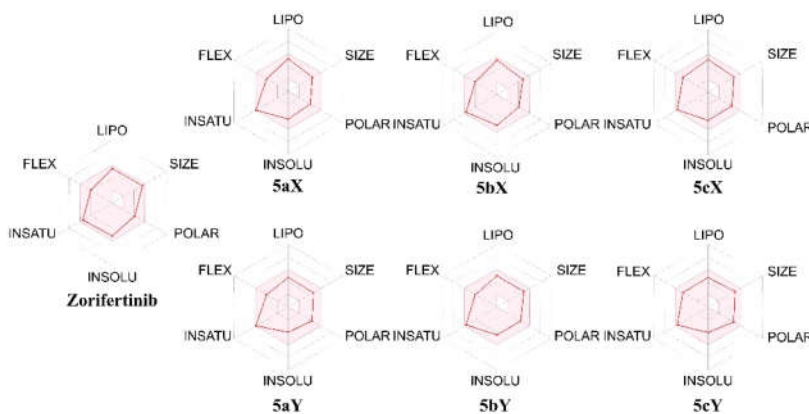


Figure 3. The bioavailability radar chart of Zorifertinib and its derivatives.

The specific physical and chemical parameters of target compounds are shown in Table 5, all of the compounds obeyed Lipinski's five rules and showed high gastrointestinal absorption. According to the predicted results, the oral bioavailability scores of all compounds are 0.55, which

are the same as that of control drug Zorifertinib (0.55). It can be seen from the bioavailability radar chart (Figure 3) that the synthesized Zorifertinib derivatives had excellent physicochemical parameters, and the evaluated drug properties (such as polarity, lipophilicity, solubility, etc) were all within the reasonable range. Therefore, the synthesized derivatives could be considered as drug-like molecules, which were worthy for further study and exploration.

Table 5. Physicochemical properties and ADME properties of target compounds.

Compd.	MW (g/mol) <500	Rotatable bonds	H-bond acceptors <10	H-bond donors <5	TPSA (Å ²) ≤140	Log P _{ow}	^a Log S	^b GI	Violation Lipinski Rule of 5	^c BS
5aX	364.40	6	5	1	76.58	2.66	-4.43	High	0	0.55
5bX	396.41	6	6	1	76.58	3.26	-4.89	High	0	0.55
5cX	394.42	7	6	1	85.81	2.10	-4.51	High	0	0.55
5aY	380.40	6	6	1	85.81	1.87	-3.98	High	0	0.55
5bY	412.41	6	7	1	85.81	2.47	-4.44	High	0	0.55
5cY	410.42	7	7	1	95.04	1.32	-4.05	High	0	0.55
Zorifertinib	459.90	6	7	1	79.82	3.17	-5.26	High	0	0.55

^aLog S-the water solubility of the compound. ^bGI-gastrointestinal absorption. ^cBS-bioavailability score.

CONCLUSION

In this work, a series of novel 4-arylaminquinazoline derivatives were synthesized, and the structure of compound **5aX** was analyzed by single crystal X-ray diffraction. The antitumor activity of the target compounds *in vitro* was evaluated by CCK-8 method, with Zorifertinib as the positive control. The IC₅₀ of compound **5cX** on A549 and H1975 was tested and showed a good inhibitory effect on cell line A549 (IC₅₀ < 2.5 μM) and cell line H1975 (IC₅₀ < 2.5 μM), which is better than the positive control drug Zorifertinib (against A549: IC₅₀ = 31.08 μM; against H1975: IC₅₀ = 64.17 μM). The molecular docking of compound **5cX** with EGFR^{WT} and EGFR^{L858R/T790M} showed better inhibitory activity by hydrogen bonding, and ADME prediction indicated that compounds had good physical and chemical parameters. Further studies on structural optimization and biological activities about these derivatives are still studied in our group and will be reported in the future.

ACKNOWLEDGEMENTS

Authors wish to thank the Natural Science Foundation of Liaoning Province (20180550016) and Scientific Research Fund Liaoning Provincial Education Department of China (LJGD2020015) for providing funds for conducting this research.

REFERENCES

- Das, R.; Mehta, D.K.; Dhanawat, M. Bestowal of quinazoline scaffold in anticancer drug discovery. *Anticancer Agent Med. Chem.* **2021**, *21*, 1350-1368.
- Rivero, I.A.; Espinoza, K.; Somanathan, R. Syntheses of quinazoline-2,4-dione alkaloids and analogues from Mexican Zanthoxylum species. *Molecules* **2004**, *9*, 609-616.
- Anjleena, M.; Ranju, B.; Clarissa, E.H.; Celestial, T.Y.; Gautam S.; Alan, P.K.; Mahendra, B.; Kamalendra, Y. Novel amide analogues of quinazoline carboxylate display selective antiproliferative activity and potent EGFR inhibition. *Med. Chem. Res.* **2020**, *29*, 2112-2122.

4. Jin, H.; Wu, B.X.; Zheng, Q.; Hu, C.H.; Tang, X.Z.; Zhang, W.; Rao, G.W. Design, synthesis, biological evaluation and docking study of novel quinazoline derivatives as EGFR-TK inhibitors. *Future Med. Chem.* **2021**, *13*, 601-612.
5. Gupta, T.; Rohilla, A.; Pathak, A.; Akhtar, M.J.; Haider, M.R.; Yar, M.S. Current perspectives on quinazolines with potent biological activities: A review. *Synthetic Commun.* **2018**, *48*, 1099-1127.
6. Brullo, C.; Rocca, M.; Fossa, P.; Cichero, E.; Barocelli, E.; Ballabeni, V.; Flammini, L.; Giorgio, C.; Saccani, F.; Domenichini, G.; Bruno, O. Synthesis of new 5,6-dihydrobenzo[h]quinazoline 2,4-diamino substituted and antiplatelet/antiphlogistic activities evaluation. *Bioorg. Med. Chem. Lett.* **2012**, *22*, 1125-1129.
7. Ravez, S.; Castillo-Aguilera, O.; Depreux, P.; Goossens, L. Quinazoline derivatives as anticancer drugs: A patent review (2011-present). *Expert. Opin. Ther. Pat.* **2015**, *25*, 789-804.
8. Cai, Z. Q.; Jin, Z. S.; Jin, Z. S.; Hou, L.; Huang, G. W.; Tian, J. Q.; Wang, G. J. Synthesis of several new quinazolin-4-amines containing p-toluenesulfonate moiety. *J. Chem. Res.* **2016**, *40*, 573-575.
9. Hao, J.; Hu, G.D.; Guo, W.R. Research progress in quinazoline derivatives as multi-target tyrosine kinase inhibitors. *Heterocycl. Commun.* **2018**, *24*, 1-10.
10. Arafat, M.; Abdel-Latif, E.; El-Taweel F.M.; Ayyadl, S.N.; Mohamed, K.S. Synthesis and biological assessment of new benzothiazolopyridine and benzothiazolyl-triazole derivatives as antioxidant and antibacterial agents. *Bull. Chem. Soc. Ethiop.* **2022**, *36*, 451-463.
11. Zhang, L.; Yang, Y.Y.; Zhou, H.J.; Zheng, Q.M.; Li, Y.H.; Zheng, S.S.; Zhao, S.Y.; Chen, D.; Fan, C.W. Structure-activity study of quinazoline derivatives leading to the discovery of potent EGFR-T790M inhibitors. *Eur. J. Med. Chem.* **2015**, *102*, 445-463.
12. Ciardiello, F. Epidermal growth factor receptor tyrosine kinase inhibitors as anticancer agents. *Drugs* **2000**, *60*, 25-32.
13. Liu, Y.J.; Zhang, C.M.; Liu, Z.P. Recent developments of small molecule EGFR inhibitors based on the quinazoline core scaffolds. *Anticancer Agent Med. Chem.* **2012**, *12*, 391-406.
14. Safyah, B.B. Synthesis of novel nitrogen heterocycles bearing biological active carboxamide moiety as potential antitumor agents. *Bull. Chem. Soc. Ethiop.* **2021**, *35*, 449-459.
15. Cai, Z.Q.; Zhao, C.K.; Li, M.Y.; Shuai, X.M.; Ding, H.G.; Wang, Q.L.; Fu, J.; Jin, Z.S.; Li, S.; Zhao, L.J. Synthesis, crystal structure and biological activity of 6-(3-chloropropoxy)-4-(2-fluorophenylamino)-7-methoxyquinazoline. *J. Chem. Res.* **2019**, *43*, 97-100.
16. Bareschino, M.A.; Schettino, C.; Troiani, T.; Martinelli, E.; Morgillo, F.; Ciardiello, F. Erlotinib in cancer treatment. *Ann. Oncol.* **2007**, *18*, 35-41.
17. Han, C.; Ding, X.; Li, M.M.; Luo, N.N.; Qi, Y.X.; Wang, C.W. Afatinib, an effective treatment for patient with lung squamous cell carcinoma harboring uncommon EGFR G719A and R776C co-mutations. *J. Cancer Res. Clin.* **2022**, *148*, 1265-1268.
18. Tan, F.L.; Yang, G.Q.; Wang, Y.P.; Chen, H.B.; Yu, B.; Li, H.; Guo, J.; Huang, X.L.; Deng, Y.F.; Yu, P.X. Icotinib inhibits EGFR signaling and alleviates psoriasis-like symptoms in animal models. *Biomed. Pharmacother.* **2018**, *98*, 399-405.
19. Sun, H.; Wu, Y.L. Dacomitinib in non-small-cell lung cancer: a comprehensive review for clinical application. *Future Oncol.* **2019**, *15*, 2769-2777.
20. Meng, P.; Koopman, B.; Kok, K.; Ter Elst, A.; Schuurin, E.; Van Kempen, L.C.; Timens, W.; Hiltermann, T.J.N.; Groen, H.J.M.; Van Den Berg, A.; Van Der Wekke, A.J. Combined osimertinib, dabrafenib and trametinib treatment for advanced non-small-cell lung cancer patients with an osimertinib-induced BRAF V600E mutation. *Lung Cancer* **2020**, *146*, 358-361.
21. Tumberink, H.L.; Heimsoeth, A.; Sos, M.L. The next tier of EGFR resistance mutations in lung cancer. *Oncogene* **2022**, *40*, 1-11.
22. David, P. AZD3759 for CNS metastases in EGFR-mutant lung cancer. *Lancet Resp. Med.* **2017**, *5*, 841-842.

23. Wang, B.; Cai, Z.Q.; Shi, X.Y.; Li, X.; Li, S.; Li, J.X. Synthesis, crystal structure and anticancer activity of substituted quinazoline derivatives. *J. Chem. Soc. Pak.* **2021**, 43, 466-474.
24. Ding, H.G.; Cai, Z.Q.; Hou, L.; Hu, Z.Q.; Jin, Z.S.; Xu, D.; Cao, H.; Meng, M.M.; Xie, Y.H.; Zheng, D.Q. Synthesis and evaluation of some novel 6-substituted quinazoline derivatives as antitumor agents. *J. Chem. Soc. Pak.* **2019**, 41, 186-190.
25. Han, X.; Cai, Z.Q.; Wu, L.H.; Hou L.; Li, S. Synthesis, biological activity, and crystal structure of N,N-diethyl-2-[[7-methoxy-4-(phenylamino)quinazolin-6-yl]oxy]acetamide derivatives. *Russ. J. Gen. Chem.* **2021**, 91, 2286-2291.
26. Sheldrick, G.M. SHELXT-integrated space-group and crystal-structure determination. *Acta Crystallogr. A* **2015**, 71, 3-8.
27. Zhang, X.W.; Gureasko, J.; Shen, K.; Cole, P.A.; Kuriyan, J. An allosteric mechanism for activation of the kinase domain of epidermal growth factor receptor. *Cell* **2006**, 125, 1137-1149.
28. Hanan, E.J.; Baumgardner, M.; Bryan, M.C.; Chen, Y.; Eigenbrot, C.; Fan, P.; Gu, X.H.; La, H.; Malek, S.; Purkey, H.E. 4-Aminoindazolyl-dihydrofuro[3,4-d]pyrimidines as non-covalent inhibitors of mutant epidermal growth factor receptor tyrosine kinase. *Bioorg. Med. Chem. Lett.* **2016**, 26, 534-539.
29. DeLano, W.L.; Lam, J.W. PyMOL: A communications tool for computational models. *Abstr. Pap. Am. Chem. S.* **2005**, 230, U1371-U1372.
30. Dania, A.; Michielin, O.; Zoete, V. SwissADME: A free web tool to evaluate pharmacokinetics, drug-likeness and medicinal chemistry friendliness of small molecules. *Sci. Rep.* **2017**, 7, 42717.